

The strake vortex has merged with the wing vortex at the trailing edge for  $\alpha > 12$  deg. The circulation of the strake vortex is of the same sign as that of the wing vortex and is weaker than the latter. The coalesced process is related to the wing vortex strength; however, it is not clear what the coalesced condition is.

Figure 3 shows the formation of the trailing-edge concentrated vortex. The circulation of the trailing-edge vortex is of opposite sign to that of the strake and wing vortex, and the concentrated trailing-edge vortex will move outward and upward around the wing vortex. Because the strake vortex is weak, it can deform the trailing-edge vortex sheet only slightly, and not form another concentrated vortex (see Fig. 3a). In Fig. 3b, there exist one wing vortex and one trailing-edge vortex, similar to that produced by the delta wing (see Ref. 1, Fig. 12). The strake vortex has merged in this case.

The essential feature of the calculated flowfield is quite similar to that of Hummel's experiment. The pressure distribution at  $x = 0.7$  is underestimated in comparison with experimental results (see Ref. 2, Fig. 9). The present method can be used qualitatively to simulate roll up of complicated vortex sheets.

### References

- 1 Hummel, D., "On Vortex Formation Over a Slender Wing at Large Angles of Incidence," AGARD CP-247, Jan. 1979.
- 2 Brennenstuhl, U. and Hummel, D., "Untersuchungen über die Wirbelbildung an Flügeln mit Geknickten Vorderkanten," *Zeitschrift für Flugwissenschaften und Weltraumforschung*, Vol. 5, 1981, pp. 375-381.
- 3 Kandil, O. A., "Numerical Prediction of Vortex Cores from the Leading and Trailing Edge of Delta Wings," *Proceedings of the 12th Congress of the International Council of the Aeronautical Sciences*, Munich, Germany, Oct. 1980.
- 4 Hoeijmakers, H. W. M. et al., "Vortex Flow Over Delta and Double-Delta Wings," *Journal of Aircraft*, Vol. 20, Sept. 1983, pp. 825-832.
- 5 Sacks, A. H. et al., "A Theoretical Investigation of Slender Wing-Body Combinations Exhibiting Leading Edge Separation," NASA CR-719, March 1967.
- 6 Purvis, J. W., "Analytical Prediction of Vortex Lift," *Journal of Aircraft*, Vol. 18, April 1981, pp. 225-230.

## Determination of Subcritical Damping in CF-5 Flight Flutter Tests

B. H. K. Lee\*

National Aeronautical Establishment,  
National Research Council Canada, Ottawa, Canada

### Introduction

ONE of the fundamental tasks when investigating the flutter characteristics of an aircraft is the determination of subcritical damping values of the various modes of vibration of the aircraft structure as functions of the flight velocity and altitude. There are various methods commonly used to excite the airframe in flight flutter tests. The use of stick raps has been adopted by the Canadian Forces in their flutter clearance program of CF-5 aircraft with external stores configurations. Symmetric and antisymmetric modes of the

aircraft wing can be excited rather simply by the application of elevator or aileron pulses.

### Flight Testing of the CF-5

The test aircraft was instrumented with eight accelerometers. Four were positioned at the front and rear of the tip tanks and these were the primary ones used for flutter investigation. The remaining four accelerometers were located at the nose of the wing-mounted stores and served mainly to provide vibration data of the stores. Reference 1 gives a detailed description of the test facilities and procedures. In this Note, some results for the LAU-5003/A rocket launchers are presented. The configuration for the flight test consisted of LAU-5003/A rocket launchers carrying nineteen C14 rockets with MK 1 warheads at the outboard pylons and eleven C14 rockets with MK 1 warheads at the inboard pylons. The launchers were equipped with nose cones. The aircraft carried a 150 US gallon centerline tank and two tip tanks.

All tests were performed at an altitude of approximately 7000 ft above sea level. Lateral and longitudinal stick raps were initiated by the pilot, and the response was allowed to decay for a sufficiently long time to permit on-line analysis. Based on analytical predictions and on previous experience, four structural modes were of primary interest in the LAU-5003/A flutter tests. They were the symmetric and antisymmetric wing bending and torsional modes. To improve identification of individual modes, power spectral densities were obtained from four different linear combinations of the four accelerometer signals.<sup>1</sup> Each linear combination was aimed at enhancing the power spectrum of one of the four modes of interest, and from the power spectrum, modal frequencies and damping values were deduced.

### Determination of Damping

In transient testing using stick pulses, the excitation forces generated are frequently represented by an impulse function. The damping  $g$  is obtained from the equation

$$g = \Delta f / f_{\max} \quad (1)$$

where  $f_{\max}$  is the frequency at the peak of the response power spectral density curve and  $\Delta f$  corresponds to the width of the

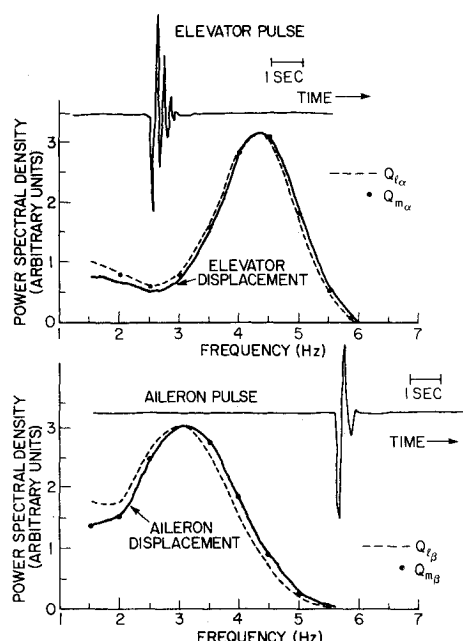
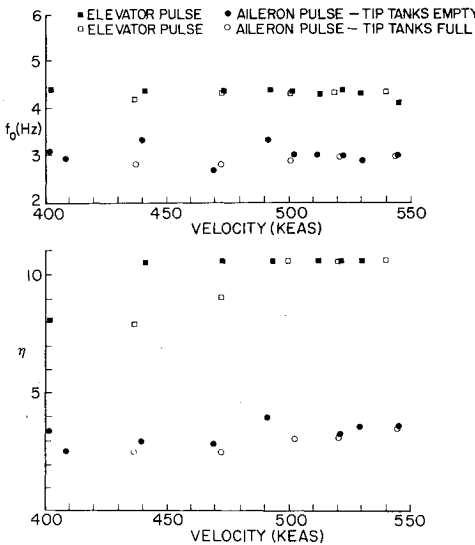


Fig. 1 Time history and power spectral density for elevator and aileron displacements.

Received Jan. 23, 1984; revision received June 22, 1984. Copyright © 1984 by B. H. K. Lee. Published by the American Institute of Aeronautics and Astronautics with permission.

\*Senior Research Officer, High Speed Aerodynamics Laboratory. Member AIAA.

Fig. 2 Variation of frequency and  $\eta$  with velocity.

curve at the half-power points. To demonstrate the accuracy of using Eq. (1) for determining damping in the CF-5 flutter tests, it is necessary to know the spectra of the excitation force and pitching moment on application of a stick rap. An approximate form of the spectral representation of the excitation force and moment is obtained by considering a typical section of the wing at 85 in. and a section of the horizontal stabilator at 50 in. from the aircraft centerline, respectively. The moment on the wing is obtained at 1/4 chord, while that on the stabilator at 0.375 chord. For a rigid fuselage, lift and moment coefficients at the stabilator can readily be transformed to those at the pitching axis of the wing. If  $\beta$  is the aileron deflection, then the Fourier component of the wing sectional force and moment can be written as

$$Q_{\ell\beta}(\omega) = qcC_{\ell\beta}\beta(\omega) \quad (2)$$

and

$$Q_{m\beta}(\omega) = qc^2C_{m\beta}\beta(\omega) \quad (3)$$

where  $q$  is the dynamic pressure,  $c$  the chord,  $\omega$  the frequency, and  $C_{\ell\beta}$  and  $C_{m\beta}$  the sectional lift and pitching moment coefficients, respectively. Similar expressions can be written for the elevator pitching at an angle  $\alpha$  by replacing  $\beta$  and the subscripts with  $\alpha$  in Eqs. (2) and (3). As an example, Fig. 1 shows typical filtered time histories of the elevator and aileron displacement pulses measured from potentiometers together with their spectra. In this particular case, the flight velocity was approximately 500 KEAS. Also shown in the figure are the spectra for  $Q_{\ell\alpha}$ ,  $Q_{m\alpha}$  for the elevator pulse and  $Q_{\ell\beta}$  and  $Q_{m\beta}$  for the aileron pulse using Eqs. (2) and (3) and the experimental  $\alpha(\omega)$  and  $\beta(\omega)$  spectra. These force and moment spectra are adjusted so that their peak values correspond to those of the displacement spectra for the purpose of comparing the shape of the spectral curves. The lift and moment coefficients  $C_{\ell\alpha}$ ,  $C_{\ell\beta}$ ,  $C_{m\alpha}$ , and  $C_{m\beta}$  are calculated using a two-dimensional transonic small-disturbance unsteady computational code developed by ONERA.<sup>2</sup> It can be seen from this figure that an exponential cosine function of the form  $e^{-\alpha' t} \cos \omega_0 t$ , where  $\alpha'$  and  $\omega_0$  are the decay coefficient and frequency, respectively, is a better representation of the lift and moment than an impulse function. The power spectral density  $S(\omega)$  can be written as

$$S(\omega) = S_0 \left\{ \frac{I}{1 + \theta^2(\omega - \omega_0)^2} + \frac{I}{1 + \theta^2(\omega + \omega_0)^2} \right\} \quad (4)$$

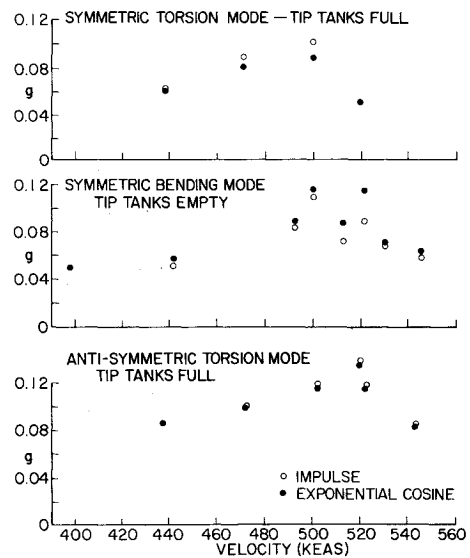


Fig. 3 Comparison of damping for impulse and exponential cosine excitation force.

where  $S_0$  is a constant,  $\omega_0$  corresponds to the frequency at the peak of the spectral curve, and  $\theta = 1/\alpha'$ . Define  $\eta = S(\omega_0)/S(0)$ , then  $\theta$  can be solved in terms of  $\eta$  and  $\omega_0$  by the following equation:

$$\theta = \frac{1}{2\omega_0} \left\{ (4\eta - 3) + \sqrt{16\eta^2 - 16\eta + 1} \right\}^{1/2} \quad (5)$$

for  $\eta \geq 0.9333$ . In the speed range from 400 to 550 KEAS where the flight tests were carried out, it was found that the shape of the power spectral density curves for the sectional force and moment were similar to those for the elevator and aileron displacements. The two-dimensional calculations at a representative section of the wing and stabilator show  $C_{m\alpha}$  and  $C_{m\beta}$  to be nearly constant in the frequency range of 1 to 6 Hz while  $C_{\ell\alpha}$  and  $C_{\ell\beta}$  do not change significantly. Values of  $\eta$ ,  $\omega_0$ , and  $\theta$  for the force and moment spectra can be approximated by those determined from the experimental displacement spectra. In evaluating  $\eta$ ,  $S(\omega_0)$  and  $S(0)$  are chosen such that a best-fit curve is obtained. Figure 2 shows that the frequency  $f_0 = \omega_0/2\pi$  for the aileron and elevator pulses can be treated to be approximately constant with aircraft speed, and independent of whether the tip tanks are empty or full. The values of  $\eta$  are also nearly the same within the range of air speeds considered, except for the elevator pulse at air speeds below 470 KEAS.

Using Eq. (4), an expression for the damping can be derived, and the detailed derivation is given in Ref. 3. Figure 3 shows the values of the damping obtained from impulse and exponential cosine excitation forces. The difference in damping increases with the value of  $g$  and is more noticeable for the symmetric than the antisymmetric modes. This is due to the larger values of  $\eta$  and hence  $\theta$  for the elevator pulses, which are nearly thrice bigger than those for the aileron pulses as shown in Fig. 2.

### Conclusions

The use of stick raps to excite the modes of vibration in CF-5 flight flutter tests is simple and quite effective. Spectral analysis of the elevator and aileron pulses shows that the time histories of the displacements can be represented by exponential cosine functions. The damping results obtained from an impulse representation of the lift and moment generated by stick raps may be quite different from those using an exponential cosine function representation. The

differences are generally larger for the symmetric modes since elevator pulses decay slower than aileron pulses and usually oscillate a few cycles before they are damped out.

### Acknowledgment

The author wishes to thank the National Defense of Canada for their support and making available the flight test data.

### References

- 1 Lee, B. H. K. and Goodey, J. H., "A Canadian Approach to Flutter Clearance for External Stores," *Recent Transonic Flutter Investigations for Wings and External Stores*, AGARD-R-703, 1983.
- 2 Coustou, M. and Angelini, J. J., "Numerical Solutions of Nonsteady Two-Dimensional Transonic Flows," *Journal of Fluids Engineering*, Vol. 101, Sept. 1979, pp. 341-347.
- 3 Lee, B. H. K., "An Interactive Computer Program for the Determination of Subcritical Damping in Flutter Flights Tests," *Proceedings of Sixth Biennial Aircraft/Stores Compatibility Symposium*, Md., 1982.

*From the AIAA Progress in Astronautics and Aeronautics Series . . .*

## INJECTION AND MIXING IN TURBULENT FLOW—v. 68

*By Joseph A. Schetz, Virginia Polytechnic Institute and State University*

Turbulent flows involving injection and mixing occur in many engineering situations and in a variety of natural phenomena. Liquid or gaseous fuel injection in jet and rocket engines is of concern to the aerospace engineer; the mechanical engineer must estimate the mixing zone produced by the injection of condenser cooling water into a waterway; the chemical engineer is interested in process mixers and reactors; the civil engineer is involved with the dispersion of pollutants in the atmosphere; and oceanographers and meteorologists are concerned with mixing of fluid masses on a large scale. These are but a few examples of specific physical cases that are encompassed within the scope of this book. The volume is organized to provide a detailed coverage of both the available experimental data and the theoretical prediction methods in current use. The case of a single jet in a coaxial stream is used as a baseline case, and the effects of axial pressure gradient, self-propulsion, swirl, two-phase mixtures, three-dimensional geometry, transverse injection, buoyancy forces, and viscous-inviscid interaction are discussed as variations on the baseline case.

200 pp., 6 x 9, illus., \$17.00 Mem., \$27.00 List

TO ORDER WRITE: Publications Dept., AIAA, 1633 Broadway, New York, N.Y. 10019